SYNTHESIS AND CHARACTERIZATION OF ALPHA ALUMINA PLATELETS AND ACICULAR MULLITE IN MgO-Al$_2$O$_3$-SiO$_2$ SYSTEM

Manuela Alejandra Zalapa-Garibay[1,2]; Ana Arizmendi-Moraquecho[2] and Simón Yobanny Reyes-López[3*]

[1]Instituto de Ingeniería y Tecnología, Universidad Autónoma de Ciudad Juárez, Av. del Charro No. 450 Nte. Col. Partido Romero C.P. 32310.

[2]Centro de Investigación de Materiales Avanzados, Alianza Norte 202. Parque de Investigación e Innovación Tecnológica, Alianza Norte, Apodaca, Nuevo León, México. C.P. 66600

[3]Instituto de Ciencias Biomédicas, Universidad Autónoma de Ciudad Juárez, Envolvente del PRONAF y Estocolmo s/n, Ciudad Juárez, Chih., México C.P. 32300.

*Corresponding author: Simón Yobanny Reyes-López

E-mail: simon.reyes@uacj.mx, yobannyr@yahoo.com.mx

Tel: +52 (656) 688-2100 Ext. 5124

Fax: +52 (656) 688-1821 Ext. 1620

Address: Envolvente del PRONAF y Estocolmo s/n, Ciudad Juárez, Chih., México C.P. 32300.

Abstract:

The search for new refractory materials, which are more reliable and less expensive, has focused research on materials like alumina and mullite, which offers a very high refractoriness. In the present work a mullite and alpha-Alumina platelets was synthesized using chemical synthesis with a relationship of raw materials $50SiO_2$-$30Al_2O_3$-$20MgO$. Alpha-Alumina platelets and mullite was obtained with reduced processing time and cost than contrasting with conventional methods. The composition, thermal analysis and microstructural evolution were followed by X-ray diffraction, differential thermal analysis and SEM microscopy. A chemical synthesis method based on the Pechini process was successfully used to synthesize alpha-alumina and acicular mullite. All synthesized precursor powders were amorphous with submicron particle size. It was found the effect of MgO in the formation of α-alumina and mullite at low temperature, α-alumina and mullite were detected after heating at 800°C and the dissolution α-alumina for the formation of secondary Mullite is around 1000°C. Finally at 1400°C is only observed well crystallized type III of secondary Mullite.

Keywords: Mullite, Alumina, Microstructure.

The authors declare that there is no conflict of interests regarding the publication of this article

Introduction

Presently ceramics, refractories, glass ceramics and also composite materials based on the system MgO-Al_2O_3-SiO_2 receive increasing value among materials for new fields of engineering. Goods made from these materials possess a low and even a negative coefficient of thermal expansion, a high mechanical strength, and a high thermal and chemical resistance [1].

The morphology and stoichiometry of mullite may be obviously influenced by the starting materials and processing technique. It is known, for example, that stoichiometric mullite $3Al_2O_3 \cdot 2SiO_2$ only forms from oxide precursors at high temperatures, whereas non

stoichiometric $2Al_2O_3 \cdot SiO_2$ mullite derives only from melt-derived systems. The mullite precursor unstable spinel phase transforms into orthorhombic mullite at 1075^0C. Furthermore, the chemical nature of precursory phases can modify the temperature of mullite formation. In porcelain bodies, primary mullite can form on the surface of kaolinite relicts that in turn serves as a seed for the crystallization of the secondary mullite needles as alkali diffuses out of feldspar at higher temperatures. As the temperature increases, the grain growth from liquid phase overlaps the dissolution of mullite grains and a bimodal microstructure develops, with an increasing fraction of large tabular grains (acicular mullite) [2,3]. Tertiary mullite has been reported in aluminous porcelains precipitating out of alumina-rich liquid. The starting compositions, and especially the alumina/silica ratio, determine the evolution of mullite crystals growth. Furthermore, the mullitisation reaction process is accomplished at lower temperatures if the proportion of alumina in the sample is above the stoichiometric composition of mullite. On the other hand, if the alumina content is too high, the excess alumina might undergo structural rearrangements and give rise to the formation of α-alumina ($α-Al_2O_3$) [2,3].

Alumina is an advanced material with microelectronic and structural applications, as well as in the technology for thermonuclear fusion reactors. Alumina is an important technical ceramic, extensively used in microelectronics, catalysis, refractories, abrasives and structural applications. Especially, high quality corundum polycrystalline materials are used as electronic substrates and as bearings in watches and in various high precision devices [4]. The $α-Al_2O_3$ is particularly stable thanks to the selective position of oxygen sublattice in octahedral sites instead of being in both tetrahedral and octahedral sites as in the case of the metastable phases[5]. Alumina ceramics materials are being considered as a promising candidate for dielectric windows on high frequency heating systems due to its very low dielectric losses at high frequencies and its radiation resistance [6].

Alpha alumina ($α-Al_2O_3$) platelet is a very useful material, which exhibits high hardness, high modulus, high strength, chemical resistance, and good properties and the plate-like shape makes $α-Al_2O_3$ platelets useful as reinforcements in various composites because of the energy dissipation induced by the incorporation of platelets [7]. There are several methods for preparing $α-Al_2O_3$ platelets, for instance, Hill *et al* [8] produced $α-Al_2O_3$

platelets by calcining alumina and aluminum fluoride mixture powder. Unfortunately, fluoride required by these methods is harmful to the environment. Miao and Sorrell [9] obtained α-Al_2O_3 platelets by calcining a mixture of natural topaz and zirconia. Hashimoto and Yamaguchi [10] synthesized α-Al_2O_3 platelets using Sodium sulfate flux. However, these methods need a calcination temperature as high as 1200°C and will consume too much energy. Recently, Park et al. [11] synthesized α-Al_2O_3 platelets using flux method in 2.45 GHz microwave field; Wu et al.[12] prepared α-Al_2O_3 platelets by laser scanning alumina powders; Wei et al. [13] synthesized α-Al_2O_3 hexagonal platelets using electrostatic spray assisted chemical vapour deposition. However, these techniques require complicated equipments and high temperature[7].

Therefore, continuous efforts are being made to develop new processing routes for high quality alumina or mullite based ceramics. These efforts are partially responsible for recent developments of chemical processing approaches, especially for advanced ceramic applications [4-7]. Available experimental data on the thermodynamic properties of the system MgO-Al_2O_3-SiO_2 at high temperatures are not numerous. They are mainly limited to the results of studying the system under consideration by methods of exchange equilibria. Thermodynamic properties of components and phase equilibria in the system MgO-Al_2O_3-SiO_2 is of a significant interest [1]. According with literature it is necessary to more experimental data for the phase equilibrium in the system MgO–Al_2O_3–SiO_2. In this work, a simple and cost-effective method was developed to synthesize single-crystal α-Al_2O_3 platelets and acicular mullite at a relatively low temperature.

Experimental Procedure

Synthesis of the alumina and mullite powders

Synthesis of the alumina and mullite powders has been prepared following the conventional Pechini synthesis process. Aluminum oxide, silicide oxide and magnesium oxide were dissolved in 10 ml of hydrofluoric acid, and then citric acid was added during stirring. The required amount of propylene glycol was then added to the solution and heated up to 70 °C for 2 hours and pH was adjusted to 9 with ammonium hydroxide. The resultant suspension was dried by spray drying technique to reduce synthesis time and obtain homogenous

powders. The resultant powder was calcined in the range of 100 to 1400°C on a conventional resistance furnace to obtain the powders.

Synthesis of alumina–mullite composite

A novel synthesis of the mullite–alumina composite was performed using silica SiO_2 (nanoparticles 99.9%, 20-60 nm, SkySpring Nanomaterials, Inc.), alumina α-Al_2O_3 (*0.3 microns, 99.9 %, Leco corporation*) and magnesita powders (nanoparticles 99.9%, 20-60 nm, SkySpring Nanomaterials, Inc.). The mole fraction of α-Al_2O_3:SiO_2:MgO was kept at 20:50:20.

First the powders were mixed in planetary ball milling (Restch PM 400) at a rate of 350 rpm for 45 minutes. Then the mixture completely was press at 2 atm (MTI: YLJ-40TA). Poly vinyl alcohol (PVA) and Tiron were used as an organic binder. The composite was kept in an oven at 80 C for drying and then the composite precursor were sintered at 1000, 1100, 1200, 1300 and 1400 C at a heating rate of 10°C/minute for 2 h soaking in a muffle furnace under air atmosphere.

The compositional and structural study of the obtained powders and composite after being heated at 1400°C was achieved by means of the following techniques. Thermogravimetry (TGA) and Differential Scanning Calorimetry (DSC) was carried out in a New Castle instrument Model Q600, to evaluate the thermal decomposition in air from 100 to 1400°C at 10°C/min, with 100 cm^3/min air gas flows. The samples were dried for 48 h in air and then at 200^0C for 24 h in an electric furnace. After this period, the weight did not change. The specimens heating was carried out with rates of 10 K/min, to 400, 600, 800, 1000, 1100, 1200, 1300 and 1400^0C and kept at the maximum temperature for 60 minutes and cooling rates were also 10 °C /min.

The crystalline evolution as a function of temperature was investigated by X-ray diffraction (Empyrean, Panalytical with CuKa radiation). A Jeol JSM-6010 SEM, at 20 kV coupled with an EDX detector (Bruker AXS Inc. XFlash 4010), was used for microstructural observations in order to distinguish the various phases and their chemical composition. An

Alpha Platinum series FT-IR (Bruker Optics Inc), was used to obtain infrared spectra by ATR technique (with diamond crystal), spectra were accumulated over 64 scans at 2 cm^{-1}.

Results and discussion

Fig.1 shows the TGA and DSC behavior. In TGA a significant weight loss in a temperature range of 25°C to 450°C is seen, weight loss is attributed to water and decomposition of organic compounds for the reactions of Pechini method. In the range of 450°C to 1050 °C, a weight loss of 10% is observed for the decomposition of AlF_3 and Mg_2SiO_4 to form Alumina and mullite, in the range temperature of 1050° C to 1350°C, a reflecting warp weight gain is observed, which is indicative of an oxidation reaction of all the metals present. Finally, in 1350°C to 1500°C a slight weight loss is observed due to structural rearrangement of α-Al_2O_3 and mullite.

Analysis of Differential Scanning Calorimetry presented in Figure 1, reflecting the decomposition of organic compounds having two endothermic peaks at a temperature of 350°C and 450°C, one exothermic peak at 1150 corresponding to the crystallization of α-Al_2O_3, and finally, the endothermic peak observed at a temperature of 1400°C probably represents the dissolution temperature for alumina crystal growth of mullite secondary type III. In order to observe in detail the phase transitions, the powders were exposed to a heat treatment at 600 °C. Figure 2 shows in DSC an endothermic peak at 750 °C, attributed to the formation of α-Al_2O_3 and primary mullite, ending in tertiary mullite at 1300°C according with DRX and SEM micrographs. The TGA in Figure 2 show a first weight loss to 400 °C for the absorbed water, a weight loss of ~ 7% due to crystallization of alumina and finally a 1% weight loss associated with the formation of mullite according whit DRX data.

The XRD of the fired samples and the corresponding indexation patterns are shown in Fig. 3. At 100°C and 200°C two phases were identified: $(NH)_3AlF_6$ and $(NH_4)_2(SiF_6)$ (crystallographic record number 01-076-0117 and 01-089-4113 respectively); at 400°C begins the formation of oxides of transition metals that are presents in raw materials (Al, Si and Mg), the Mg_2SiO_4 and AlF_3 phase are formed (with card number and crystallographic

01-074-1683 and 00-043-0435 respectively). The effect of MgO is observed in the formation of α-alumina and mullite at low temperature (cards 01-074-1081 and 98-02-8246 respectively). At 800°C stars the formation α-alumina and mullite, in the beginning the proportion of alumina is larger than mullite. At 1200°C crystalline α-Al_2O_3 platelets and some mullite crystals were also found and the increment of temperature serves to dissolution of the α-Al_2O_3 to form mullite, and finally at 1400 °C, α-Al_2O_3 is present in lower proportion than mullite crystals.

Phase evolution upon firing (25-1400°C) can be systematically followed by IR analysis as shown in Fig.4 and characteristics bands of the precursors and final phases are shown in table 1. In the range of 25 to 200°C a broad band is observed at about 3200 cm^{-1}, which is typical of the O–H stretching. The presence of two bands at about 2870 cm^{-1}, which corresponds to C–H stretching, and at 1420 cm^{-1} due to C–H bending vibration related with the citrate ions. The band ranged about 1780 cm^{-1} is reported to agree to the carboxilate anion (COO $^-$) stretching mode (a covalent carbonyl bond). The last clear band observed is ranged at about 1680 cm^{-1} and can be assigned to the antisymmetric COO$^-$ stretching mode for a bridge-type complex, as well as the band over 1120 cm^{-1} is related to ester bonds type.

Although the IR spectrum at 200°C presents similar bands as that at 100°C, the decreasing intensity clearly establishes the gradual loss of water and the citrate and carboxylate groups. It is worth noticing the wide band appearing between 500 and 900 cm^{-1}. This region corresponds to the vibrational frequencies of coordinated O–Al–O bonds, and begins to take importance at relative low temperatures. Up to 400°C the pyrolysis process continues as it is demonstrated by the strong intensity decreasing of the carboxylate anions and organic chain bands. The typical bands for the carboxylate anions have disappeared at ~400 °C, and only a trace of the carboxylate ions band remains at this temperature. These results suggest that most of the organic chains break down between 300 and 450 °C according with DSC and TGA data.

The band ranged at about 500–1100 cm^{-1} kept gaining intensity. Characteristic alumina band appear at 400^0C, in the 627 cm^{-1} corresponding to the tetrahedral Al^{iv}-O vibrations. The wide band, corresponding to the Al–O bonds for α-Al_2O_3, develop in three bands at 622, 545 and 500 cm^{-1} as temperature increases up to 800°C. The characteristic mullite

bands also appear at 800^0C, for the 1143, 827 and 735 cm^{-1} spectral region corresponding to the tetrahedral Al^{iv}-O bands. The Si-O bands appear in the 1131, 1105 and 979 cm^{-1}. At 1200 °C, the strong and well defined IR bands observed for Al–O bondings must be explained taking into account the pure XRD reflections of α-alumina observed. The mullite bands show an increasing amount of the mullite phase up to 1300^0C and higher definition of these bands is observed at 1400^0C.

The microstructure details of the samples were studied by SEM as shown in Fig.5. The obtained mullite crystals present a small globular and an acicular form, whereas the α-alumina are recognized by their hexagonal plates in the micrographs of samples at 800°C. According to DRX data, an excellent crystallization of the α-alumina occurs with the increment of temperature up to 1200°C. On the other hand, the higher mullitization in acicular form is achieved at higher temperature (> 1200 °C). The Fig.5 shows the dissolution of alumina in the range 1200-1400^0C as well as acicular mullite appearance. In the elemental mapping of samples, where one can observe that oxygen, aluminum is uniform throughout the α-aluminum oxide plates at 800°C; and oxygen, aluminum and silicon distribution for pure mullite at 1400°C.

The X-ray and the electron microscopy showed two crystalline phases, mullite needles and α-aluminum oxide plates were obtained. In chemical processes, as the sol–gel method, it is possible to obtain the same result. However, the cost of sol–gel route is higher than the one proposed here by the use of alcoxides as precursors. The products obtained by this synthesis route, based on chemicals routes, are located in the solid solution region of the phase diagram of mullite–corundum [1] and mullite–corundum-magnesium oxide (Fig.6). From this diagram, it is also deduced that this material will probably maintain its refractory properties up to 1832 °C. According whit the diagram of mullite–corundum if the temperature it is increased up to l832 °C probably be formed only alumina.

In the case for mullite–corundum-magnesium oxide composite the Fig.1 shows the TGA and DSC behavior. In TGA a significant weight loss in a temperature range of 25°C to 650°C is seen, weight loss is attributed to water and decomposition of binder. In the range

of 650°C to 1500 °C, a final weight loss of 7% is observed for the formation of Alumina and mullite, in the range temperature of 1050° C to 1350°C, a reflecting warp weight gain is observed, which is indicative of an oxidation reaction. Finally, in 1300°C to 1500°C a slight weight loss is observed due to structural rearrangement of α-Al_2O_3 and mullite. Analysis of Differential Scanning Calorimetry presented in Figure 7, reflecting the decomposition of organic compounds having tree endothermic peaks at a temperature of 100 °C, 250 °C and 350 °C, one endothermic band attributed to the formation of α-Al_2O_3 and primary mullite, one exothermic peak at 1250 °C corresponding to the crystallization of α-Al_2O_3, and finally, the endothermic peak observed at a temperature of 1350°C probably represents the dissolution temperature for alumina crystal growth of mullite secondary type III, according with DRX and SEM micrographs.

The XRD of the fired composite and the corresponding indexation patterns are shown in Fig. 8. At 1000°C stars the formation α-alumina and is well crystallized at 1100 °C, crystalline α-Al_2O_3 platelets and some mullite crystals were also found and the increment of temperature serves to dissolution of the α-Al_2O_3 to form mullite at 1300 °C, and finally at 1400 °C, α-Al_2O_3 is present in lower proportion than mullite crystals.

The microstructure of the composite was studied by SEM as shown in Fig.9. The obtained mullite crystals are present in acicular form, whereas the α-alumina is recognized by the relicts of hexagonal plates in the micrographs of samples at 800°C. According to DRX data, an excellent crystallization of the α-alumina occurs with the increment of temperature up to 1200°C. On the other hand, the higher mullitization in acicular form is achieved at higher temperature (> 1200 °C). The micrographs show the dissolution of alumina in the range 1200-1400^{0}C as well as acicular mullite appearance. In the elemental mapping of samples, where one can observe that oxygen, aluminum is uniform throughout the α-aluminum oxide plates at 800°C; and oxygen, aluminum and silicon distribution for pure mullite at 1400°C.

Conclusions

The thermal stability α-Al$_2$O$_3$ and mullite resulted at lower temperature with metalorganic precursor. Using the proposed synthesis route, it is possible to obtain mullite needles and α-aluminum oxide plates at 800°C, and pure mullite at 1400°C in 2 hours, which is considerably less energy demanding. The effect of MgO in the formation of α-alumina and mullite at low temperature were detected. The present route seems to be a good alternative for the ceramic processing, whit special characteristics of products such as high purity, homogeneity, crystallinity and it is more efficient in terms of energy consumption.

Acknowledgements

Referencias

1. V. L. Stolyarova, S. I. Lopatin, & O. B. Fabrichnaya, Thermodynamic Properties of silicate glasses and melts: VIII. System MgO-Al$_2$O$_3$-SiO$_2$. Russian J. Gen. Chem., 81, 10, 2051-2061, (**2011**).

2. S. Y. Reyes-López, J. Rodríguez-Serrato, S. Suguta-Sueyoshi, Microstructural characterization of sanitaryware, the relationship spinel and mullite. J. Ceram. Proc. Res., 14, 4, 492-497, (**2013**).

3. S. Y. Reyes-López, J. Rodríguez-Serrato, Microstructural characterization of sanitaryware by infrared and Raman spectroscopy, the role of vitreous matrix on propierties. J. Ceram. Proc. R., 16, 1, 162-168, (**2015**).

4. S. Y. Reyes-López, J. Rodríguez-Serrato, S. Suguta-Sueyoshi, Low-temperature formation of alpha alumina powders via metal organic synthesis. AZo J. of Mat. Online, 2, (**2006**).

5. S. Y. Reyes-López, R. Saucedo-Acuña, R. López-Juárez, & J. Rodríguez-Serrato, Analysis of the phase transformation of aluminum formate Al (O2CH) 3 to α-alumina by Raman and infrared spectroscopy. J. Ceram. Proc. R., 14, 5, 627-631, (**2013**).

6. M. T. Hernández, & M. González, Synthesis of resins as alpha-alumina precursors by the Pechini method using microwave and infrared heating. J. E. Ceram. Society, 22, 16, 2861-2868, (**2002**).

7. X. Su, & J. Li, Low temperature synthesis of single-crystal alpha alumina platelets by calcining bayerite and potassium sulfate. J. Mater.s Sci. Tech., 27, 11, 1011-1015, (**2011**).

8. R.F. Hill, R. Danzer and R.T. Paine, Synthesis of aluminium oxide platelets, J. Am. Ceram. Soc., 84, 514. (**2001**).

9. X. Miao and C.C. Sorrell, Alumina Platelets from Topaz–zirconia Mixtures. J. Mater. Sci. Lett., 17, 2087, (**1998**).

10. S. Hashimoto and A. Yamaguchi, Synthesis of α-Al_2O_3 platelets using sodium sulfate flux, J. Mater. Res., 14, 4667, (**1999**).

11. H.C. Park, S.W. Kim, S.G. Lee, J.K. Kim, S.S. Hong, G.D. Lee and S.S. Park: Mater. Sci. Eng. A, 363, 330, (2003).

12. Y. Wu, K.L. Choy and L.L. Hench: J. Am. Ceram. Soc., 87, 1606, (**2004**).

13. M.Wei, D. Zhi and K.L. Choy: Nanotechnology, 17, 181, (**2006**).

Table 1. Band positions in the infrared spectra of porcelain phases.

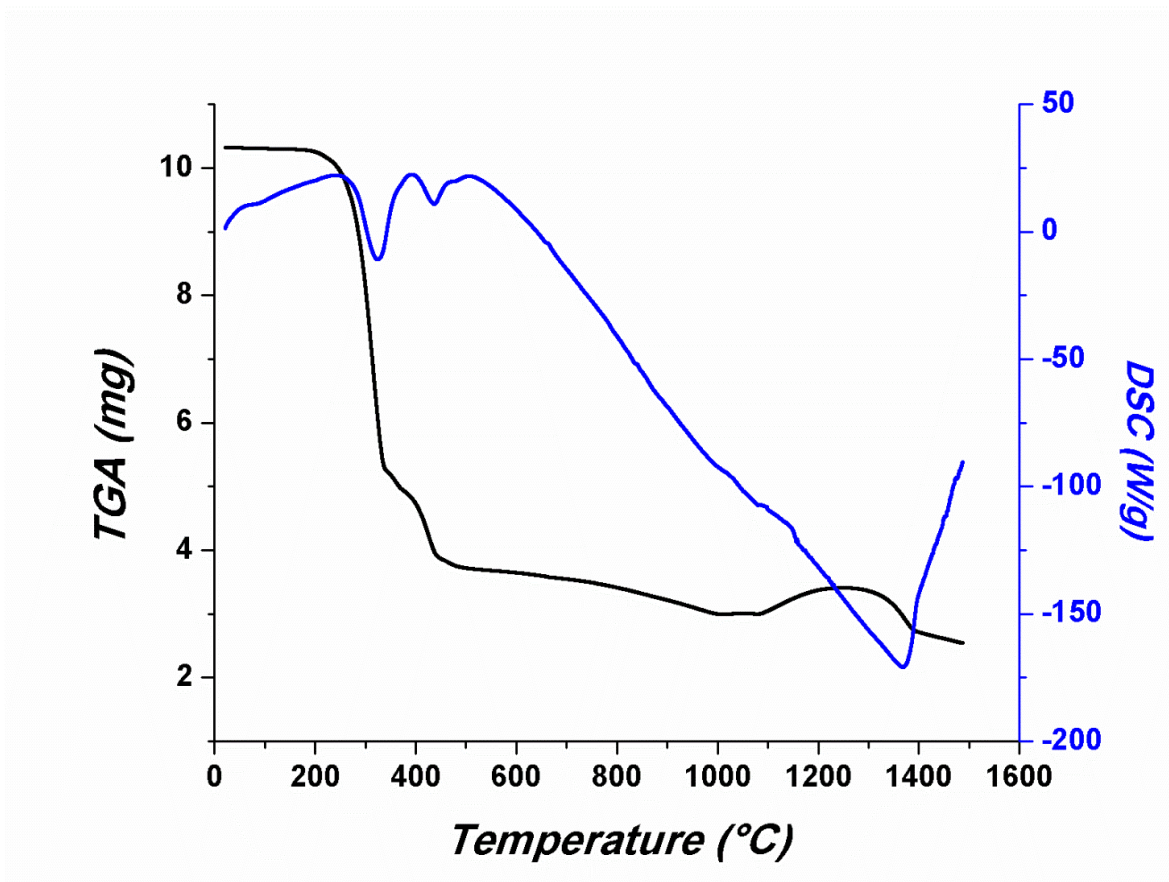| Structure	Wavenumber (cm^{-1})	Assignment	Structure	Wavenumber (cm^{-1})	Assignment
Mullite	**1143**	**Aliv-O vs**	**Mullite**	**827**	**Aliv-O vs**
Mullite	**1131**	**Si-O vs**	**Mullite**	**735**	**Aliv-O-Aliv vb**
Mullite	**1105**	**Si-O vs**	**Mullite**	**827**	**Aliv-O vs**
Alumina	**627^{-1}**	**Alvi-O vs**	**Alumina**	**545^{-1}**	**Alvi-O**
Alumina	**622^{-1}**	**Alvi-O**	**Alumina**	**500^{-1}**	**Alvi-O**

Figure Captions

Fig.1. TGA and DSC curves of experimental sample up to 1500^{0}C, with rate of 10 K/min.
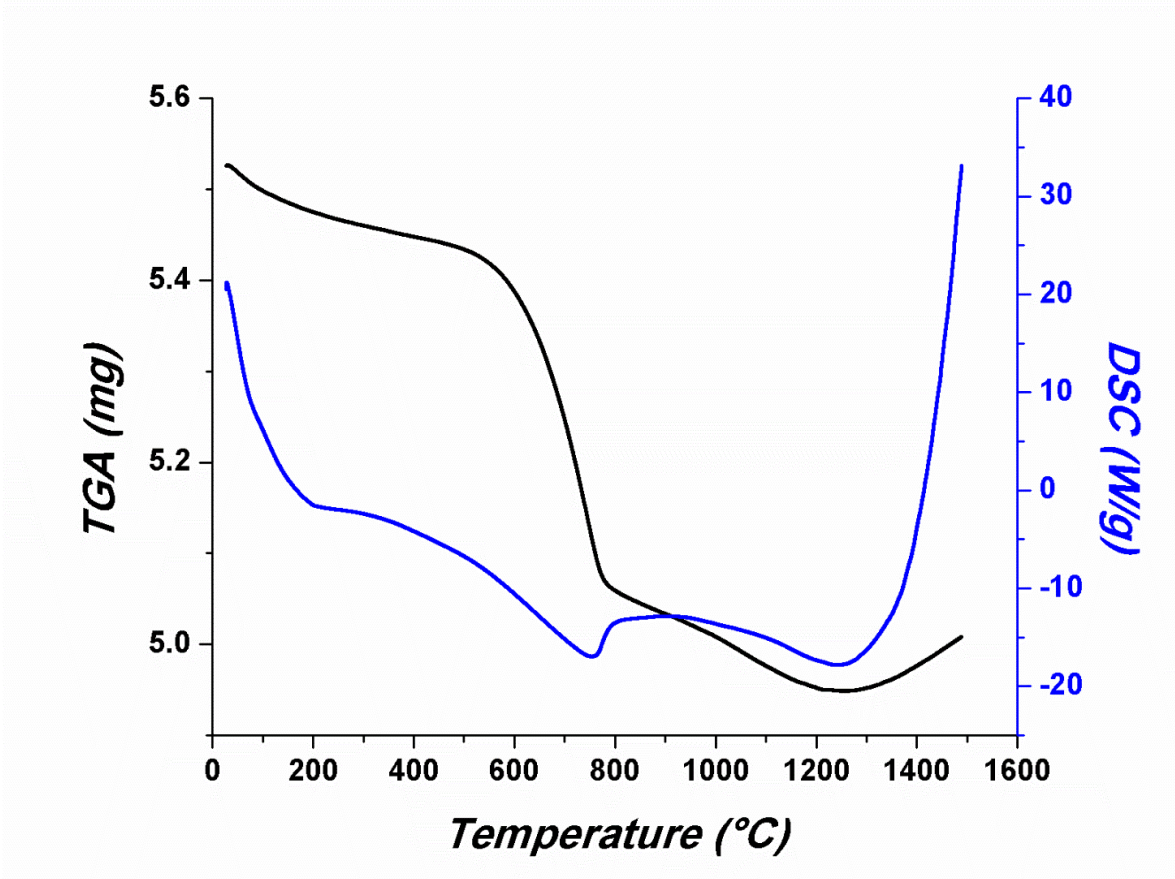
Fig.2. TGA and DSC curves of experimental sample with heat treatment at 600 °C, with rate of 10 K/min up to 1500^0C.
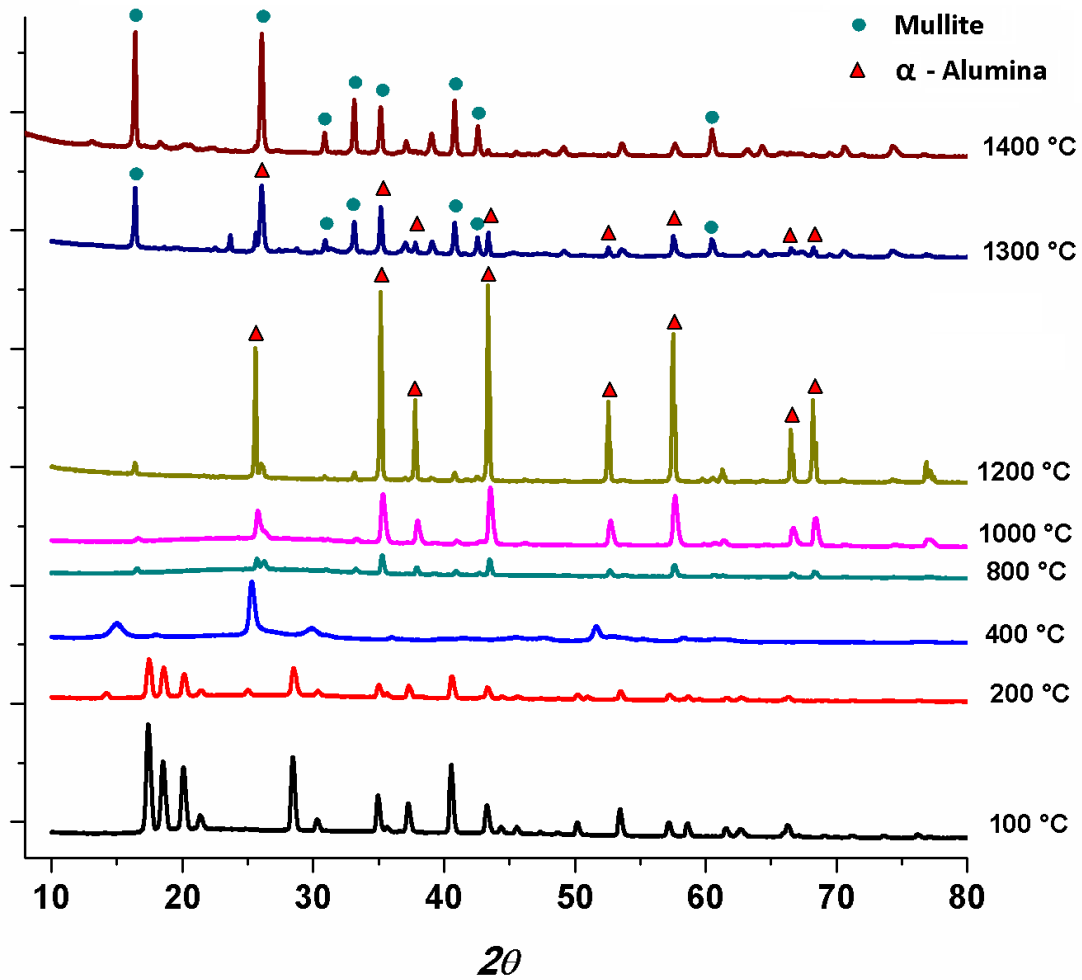
Fig.3. XRD patterns of experimental sample with heat treatment at 100, 200, 400, 800 600, 800, 1000, 1200, 1300 and 1400^0C.
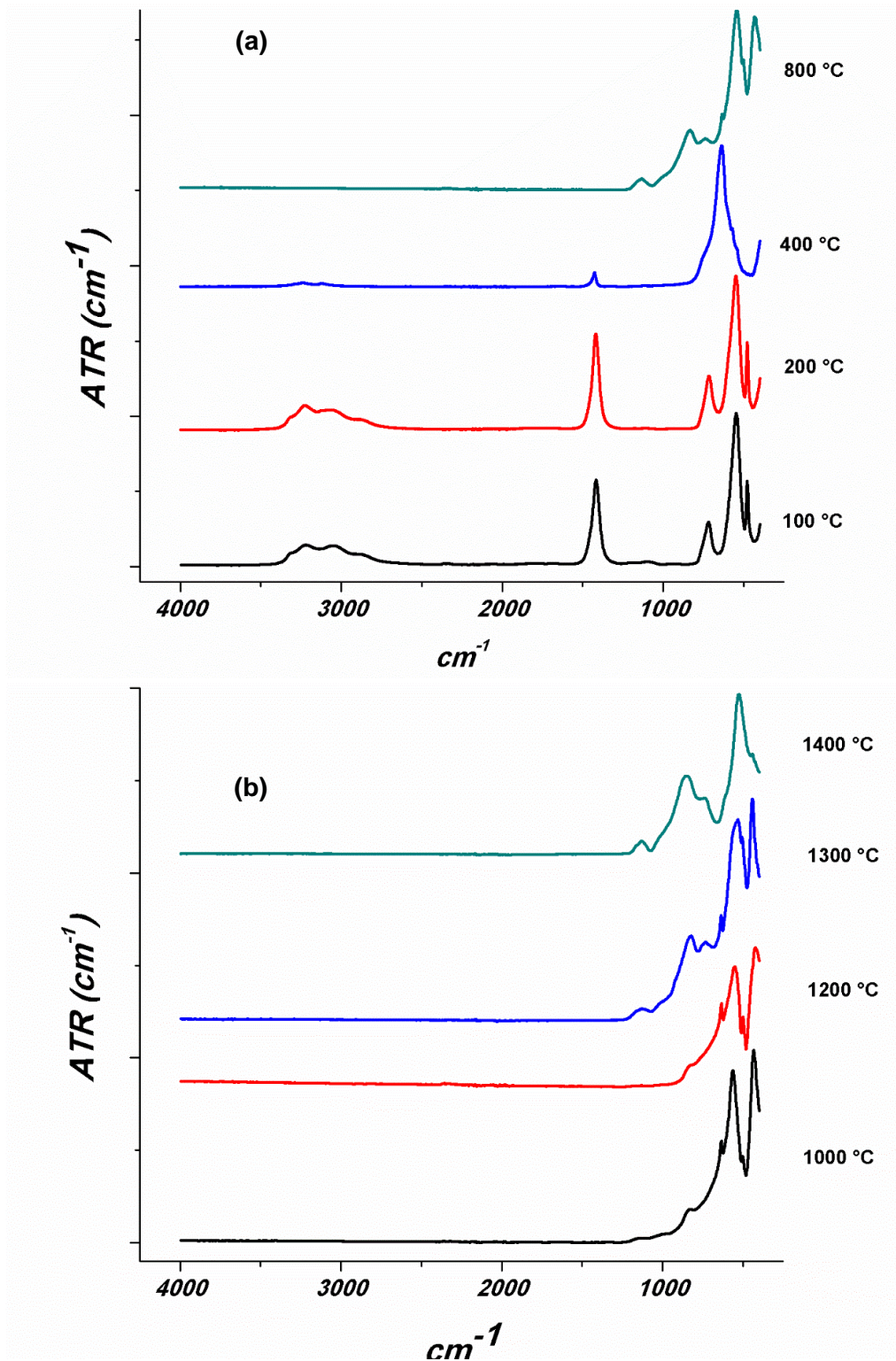
Fig.4. Infrared spectra of experimental sample with heat treatment: a) 100, 200, 400, 800 600 and 800^0C, and b) 1000, 1200, 1300 and 1400^0C.
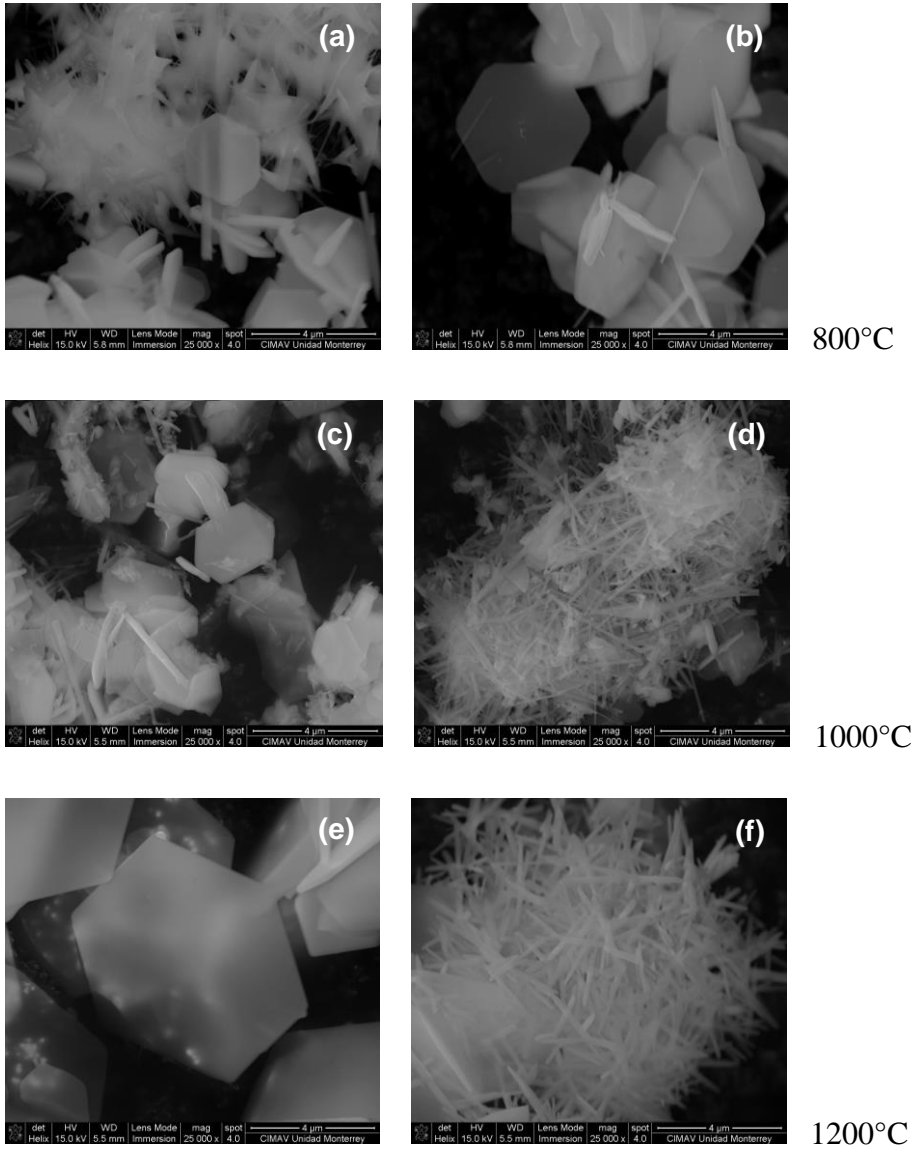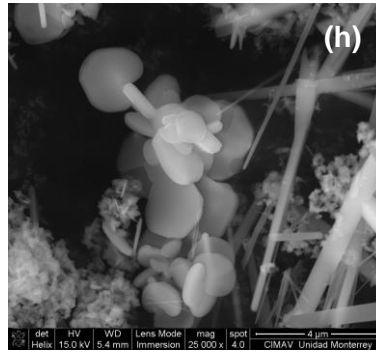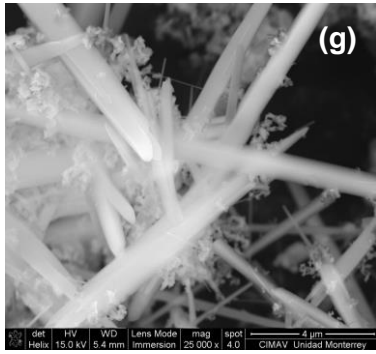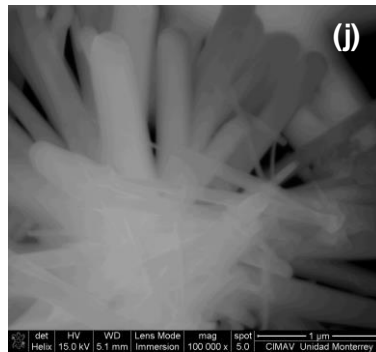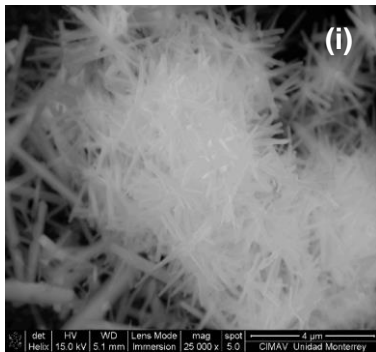
Fig 5. SEM showing mullite and alumina a) 800°C, b) 1000°C, c) 1200°C, d) 1300°C and e) 1400°C

1300°C

1400°C

Fig 5 (Continuation). SEM showing mullite and alumina a) 800°C, b) 1000°C, c) 1200°C, d) 1300°C and e) 1400°C

Al$_2$O$_3$ - SiO$_2$ - MgO
Projection (ASlag-liq), 1 atm

Al$_2$O$_3$

FactSage™

T(min) = 1362.05 °C, T(max) = 2824.73 °C

▲ Al$_2$O$_3$ - SiO$_2$ - MgO

20:50:30

T °C
2850
2600
2350
2100
1850
1600
1350

Four-Phase Intersection Points with ASlag-liq

1: AMonoxide / ASpinel / Mg2SiO4_forsterite(s)
2: ASpinel / Al2O3_corundum(alpha(s4)) / Mullite#1
3: Mullite#1 / SiO2_Cristobalite(h)(s6) / SiO2_Tridymite(h)(s4)
4: AProtopyroxene / SiO2_Cristobalite(h)(s6) / SiO2_Tridymite(h)(s4)
5: ASpinel / Mg4Al10Si2O23_Sapphir(s) / Mullite#1
6: Mg2Al4Si5O18_Cordieri(s) / Mg4Al10Si2O23_Sapphir(s) / Mullite#
7: AClinopyroxene / AProtopyroxene / Mg2SiO4_forsterite(s)
8: Mg2Al4Si5O18_Cordieri(s) / Mullite#1 / SiO2_Tridymite(h)(s4)
9: ASpinel / Mg2Al4Si5O18_Cordieri(s) / Mg4Al10Si2O23_Sapphir(s)
10: AClinopyroxene / AProtopyroxene / SiO2_Tridymite(h)(s4)
11: ASpinel / Mg2Al4Si5O18_Cordieri(s) / Mg2SiO4_forsterite(s)
12: AClinopyroxene / Mg2Al4Si5O18_Cordieri(s) / Mg2SiO4_forsterite(s)
13: AClinopyroxene / Mg2Al4Si5O18_Cordieri(s) / SiO2_Tridymite(h)(s4)

A = Al2O3, B = MgO, C = SiO2
         X(A)   X(B)   X(C)   C
1: 0.07687 0.59349 0.32965 1645.61
2: 0.30507 0.26993 0.42500 1574.78
3: 0.14755 0.13663 0.71582 1465.40
4: 0.03081 0.40771 0.56148 1465.39
5: 0.20909 0.29312 0.49779 1463.66
6: 0.20223 0.29142 0.50635 1455.37
7: 0.04115 0.43936 0.51948 1449.18
8: 0.14894 0.15516 0.69590 1445.20
9: 0.17311 0.32597 0.50092 1440.28
10: 0.05157 0.37743 0.57101 1414.27
11: 0.10823 0.41007 0.48169 1380.64
12: 0.09507 0.40283 0.50210 1374.32
13: 0.08161 0.33651 0.58188 1362.05

Al$_2$O$_3$(s4)

ASpinel

Mullite

Mg$_4$Al$_{10}$O$_{23}$(s)
Mg$_2$Al$_4$Si$_5$O$_{18}$(s)

AMonoxide

SiO$_2$(s4)
SiO$_2$(s6)
SiO$_2$(s6)

Mg$_2$SiO$_4$(s)
AProtopyroxene
SiO$_2$(liq)

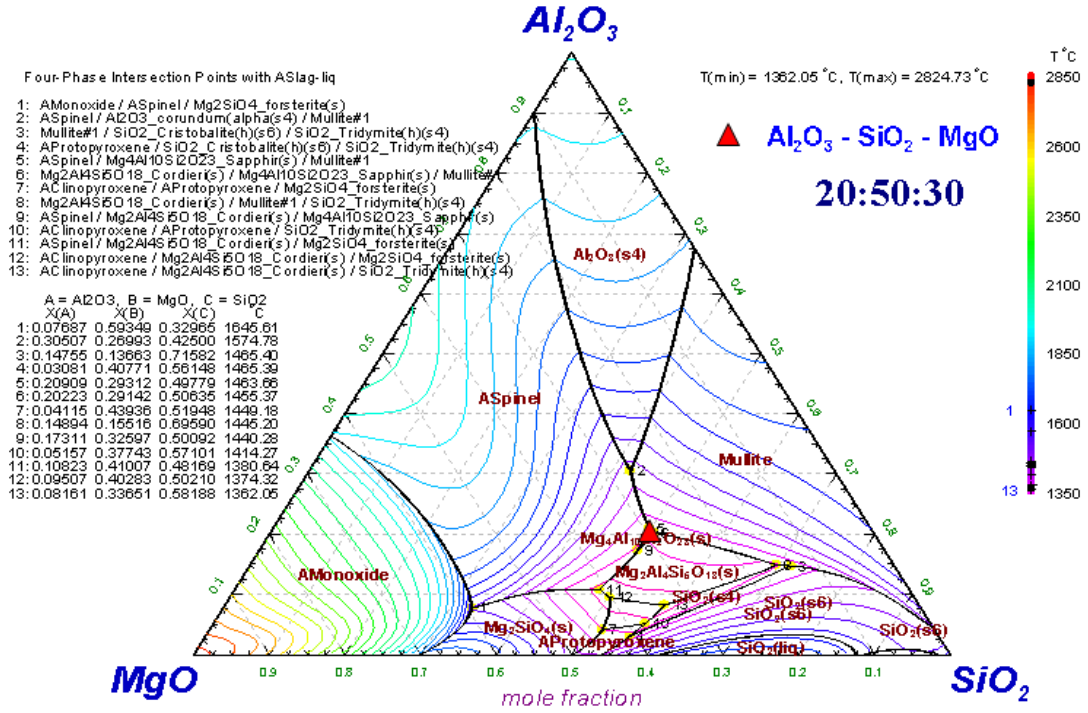MgO   0.9   0.8   0.7   0.6   0.5   0.4   0.3   0.2   0.1   SiO$_2$

mole fraction

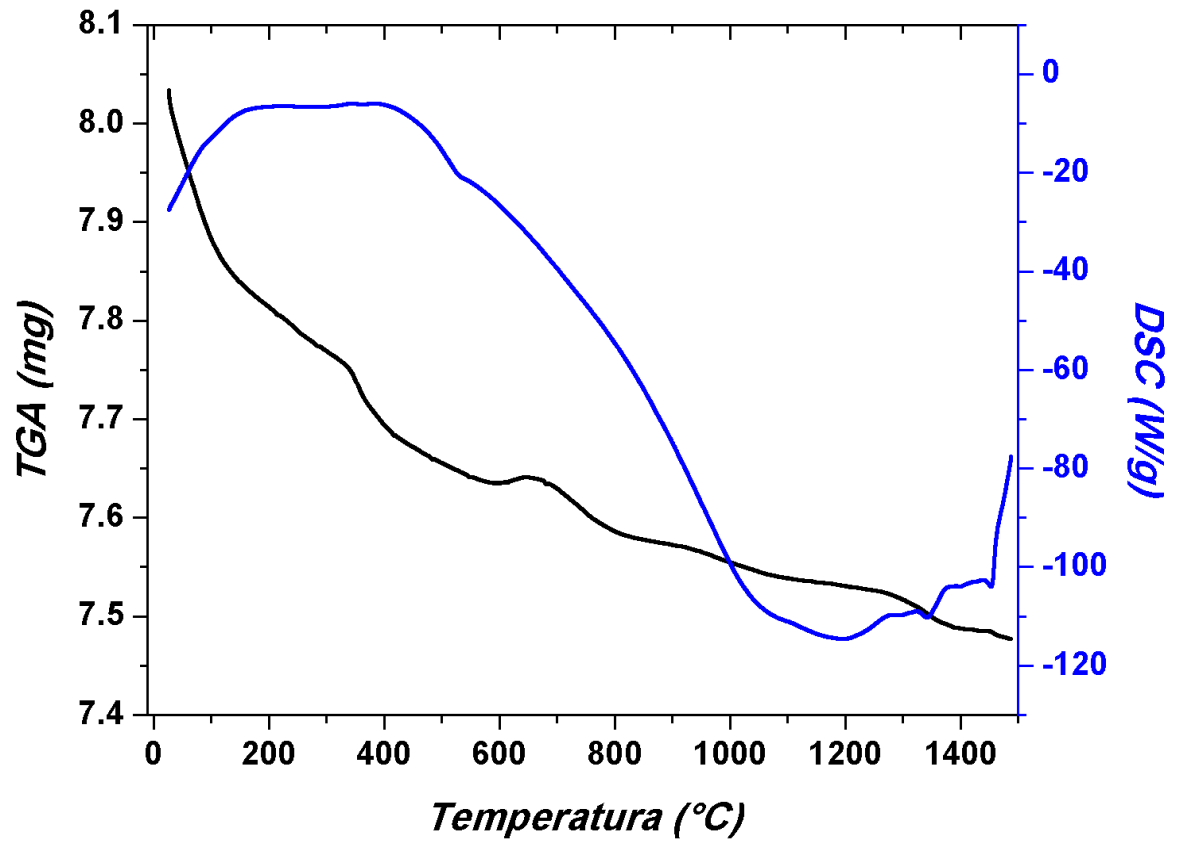Fig. 6. Mullite–corundum-magnesium oxide calculated projection by FactSage.

Fig.7. TGA and DSC curves of experimental composite sample up to 1500^0C, with rate of
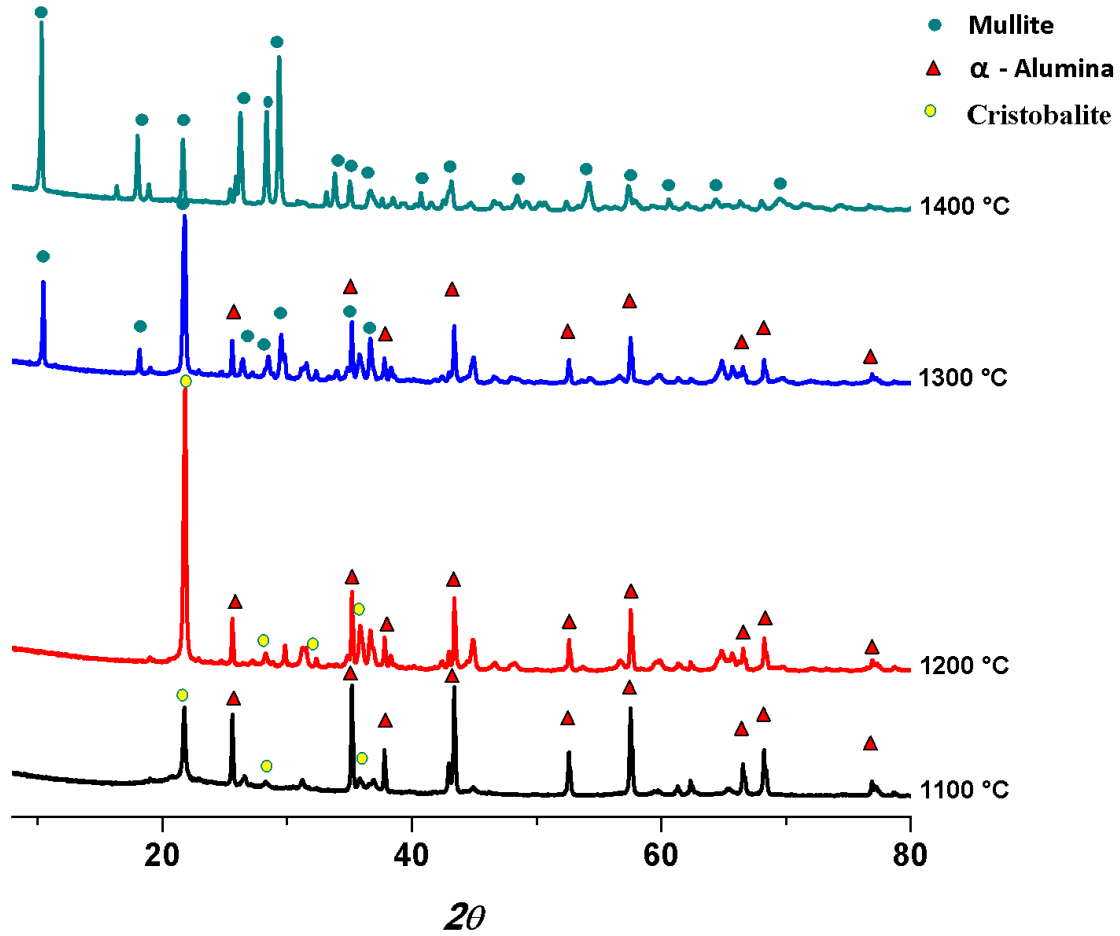10 K/min.

Fig.8. XRD patterns of experimental composite with heat treatment at 1100, 1200, 1300 and 1400^0C.
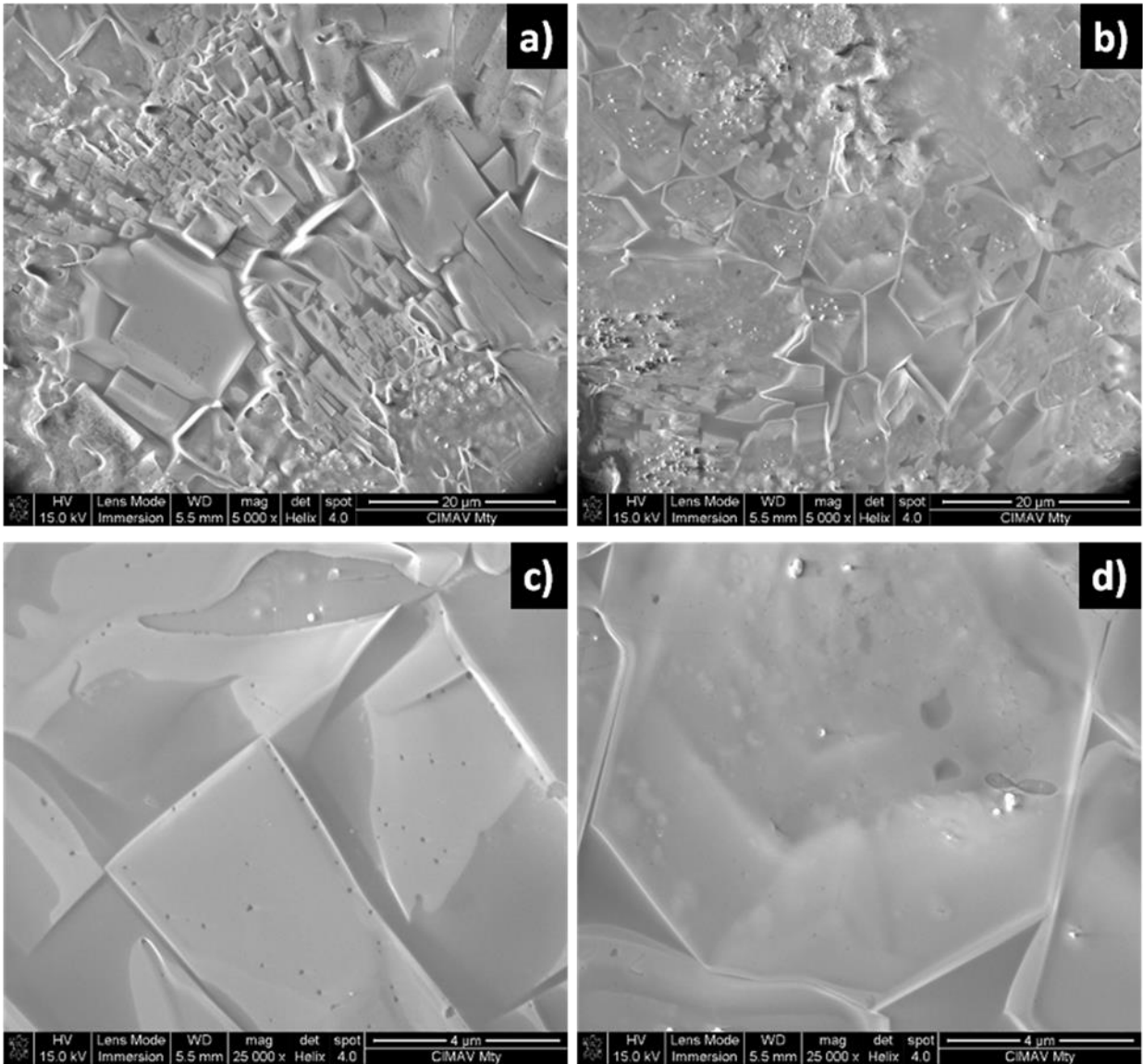
Fig. 9. SEM showing mullite and alumina at 1400°C, a) 5,000 X zone 1, b) 5,000 X zone 2, c) 25,000 X zone 1 and d) 25,000 X zone 2